Journal of Food Engineering 342 (2023) 111358

Contents lists available at ScienceDirect

Journal of Food Engineering

journal homepage: www.elsevier.com/locate/jfoodeng

Towards dry fractionation of soybean meal into protein and dietary fiber concentrates

Botagoz Kuspangaliyeva, Dinara Konakbayeva, Solmaz Tabtabaei *

Department of Chemical Engineering, Howard University, Washington, DC, USA

ARTICLE INFO

Keywords:
Tribo-electrostatic separation
Soybean meal
Protein
Fiber
Particle size

ABSTRACT

Tribo-electrostatic separation of hexane-defatted soybean flour was studied to produce protein- and fiber-rich fractions. The separation was carried out under laminar and turbulent airflow rates and plate voltages ranging from ±1 to ±6.5 kV. The combination of laminar airflow rate and high plate voltage resulted in the highest yield of protein and fiber particles with modest enrichment levels. Accordingly, the soybean flour was enriched in protein from 55.3 to 58.4% and fiber from 15.4 to 19.6%, accounting for 44.4 and 16.8% protein and fiber separation efficiencies, respectively. The distribution of protein and fiber along the negatively charged electrode showed no significant difference in terms of enrichment level. Still, more protein and fiber particles accumulated at the bottom of the electrode, according to the yield results. At 7 LPM and ±6.5 kV, a direct relationship was found between protein content and the average particle size of the fractions. In contrast, a reverse relationship was found for the fiber content.

1. Introduction

Oilseed meals are excellent sources of protein and dietary fiber. Their proteins can provide essential amino acids for human needs, either individually or as mixtures, and be utilized in different food formulations to provide superior functional properties such as gelation, foaming, and emulsification (Tabtabaei et al., 2017a). Dietary fibers can also improve the food products' sensory, viscosity, texture characteristics, and shelf-life (Mudgil and Barak, 2013). However, the existing wet fractionation methods for plant protein and fiber extraction require solvents, concentrated acids, and alkali, followed by an intensive drying step. The conventional wet fractionation technology isolates plant proteins (>90%) through solvent oil removal, protein solubilization, centrifugation, isoelectric precipitation, washing, neutralization, and freeze/spray drying, where the elevated temperatures and extreme pH shifts negatively impact protein solubility and functionality (Jafari et al., 2016; Tabtabaei et al., 2019). Other wet fractionation processes include aqueous or enzymatic aqueous extraction processes (AEP/EAEP) that can eliminate the de-oiling step of oilseeds before protein solubilization and precipitation (Tabtabaei and Diosady, 2013). However, during these AEP/EAEP processes, natural emulsifiers like oleosin protein, phospholipids, and storage proteins produce stable oil-in-water emulsions that are very difficult and challenging to demulsify to free oil (Tabtabaei et al., 2015, 2014, 2013). On the other hand, all types of wet fractionation methods require large volumes of water. As a result, they generate high biochemical oxygen demand waste streams that have a massive impact on the ecosystem (Schutyser and van der Goot, 2011; Wang et al., 2015b). The drawbacks of the wet fractionation methods provided the stimulus to explore a more sustainable approach that can preserve the compound's native properties and structure.

Air classification and tribo-electrostatic separation are the most widely applied techniques in the dry separation of plant flours. Both include the primary milling stage, followed by a dry fractionation with different driving forces. The separation under air classification is achieved due to the difference in particles' aerodynamic properties, namely size and density difference (Schutyser and van der Goot, 2011). Unfortunately, air classification technology might be inefficient for particle separation with similar physical characteristics (Tabtabaei et al., 2016a; Wang et al., 2014). Tribo-electrostatic separation works on the basic principle of imparting charges to the particles that can be further separated based on their charge difference under an external electric field. Through this process, the agro-material particles are tribo-charged based on their size, shape, and surface properties via collisions against each other and by physical contact with the wall material of the

* Corresponding author. Department of Chemical Engineering College of Engineering and Architecture (CEA) Howard University 2300 6th Street, NW, Washington, DC, 20059, USA.
E-mail address: solmaz.tabtabaei@howard.edu (S. Tabtabaei).

https://doi.org/10.1016/j.jfoodeng.2022.111358
Received 4 June 2022; Received in revised form 15 November 2022; Accepted 16 November 2022
Available online 21 November 2022

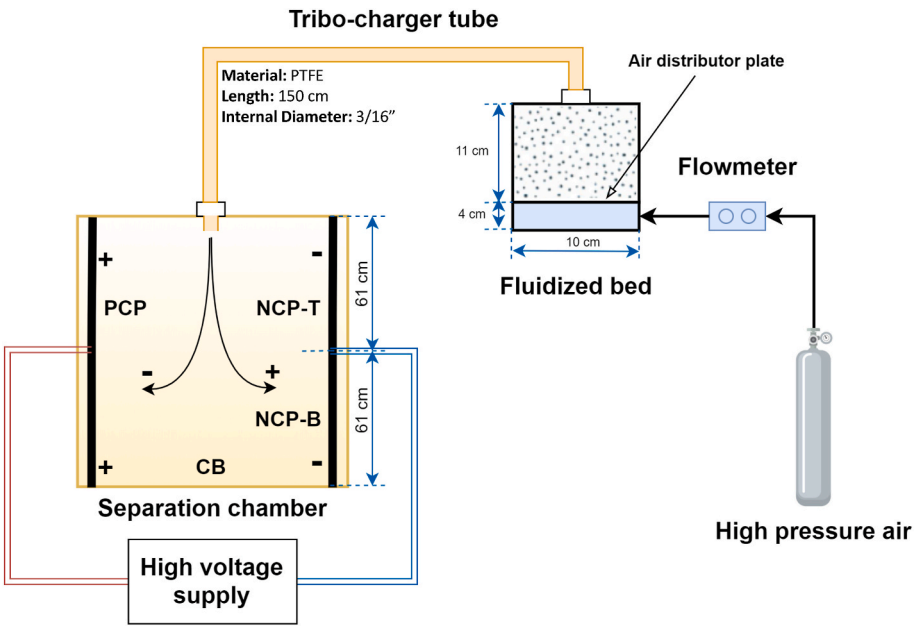

Fig. 1. Experimental set-up and schematic illustration of the tribo-electrostatic separator. "NCP-T" is the protein-rich fraction collected from the top half section of the negatively charged plate electrode. "NCP-B" is the protein-rich fraction collected from the bottom half section of the negatively charged plate electrode. "PCP" is the fiber-rich fraction collected from the positively charged plate electrode. "CB" is the fraction collected from the chamber bottom.

tribo-charger apparatus (Tabtabaei et al., 2016a; Wang et al., 2015b, 2014). For example, due to the protein's ionizable side chains, C- and N-terminal groups, plant protein particles can acquire a much higher charge than starch and dietary fibers, which have low ionizability and proton affinity (Tabtabaei et al., 2016a).

In our previous studies, the electrostatic separation approach has been mainly applied for the protein enrichment of starch-rich legumes and cereal groats, including navy bean flour (Jafari et al., 2016; Tabtabaei et al., 2019, 2017b, 2016a, 2016b) and oat groats (Konakbayeva et al., 2022; Konakbayeva and Tabtabaei, 2021). The triboelectric separation of starchy legumes reflects the distinct difference in composition of large (starch-rich) and small (protein-rich and fiber-rich) particles in finely milled flours which might not be the case for oilseed meals or cereal bran lacking starch and mainly consisting of protein and dietary fiber particles. Other research groups have concentrated on oilseed meals, including rapeseed, soybean, lupine, and cereal brans as wheat and rice bran flours (Basset et al., 2016; Wang et al., 2016, 2015b; Xing et al., 2018). For instance, pin-milled and then impact-milled lupine flour with an initial protein content of 40.5% could be converted into a protein fraction of 65.1% with a total protein recovery of 10% after two consecutive fractionation steps (Wang et al., 2016). In another study, the successive three-step tribo-electrostatic separation of rapeseed oil cake with an initial protein content of 37% and lignin content of 16% resulted in producing the protein-rich fraction with 51% protein and the lignin-rich fraction with 42% lignin (Basset et al., 2016). Another study was conducted by Xing et al. (2018) on the protein enrichment of soy flour by applying tribo-electrostatic separation with the stainless steel spiral- and slit-type charger tube. However, the influence of plate voltage and airflow rate on the separation efficiency was not considered. In addition, the application of this separation approach to simultaneous fractionation of protein and dietary fiber particles from soybean meal flours has not been investigated. Therefore, in the current study, the capability of the tribo-electrostatic separation approach was explored in the partial dissociation of protein- and fiber-enriched particles from soybean meal flour.

The detailed objectives of the present study were: (1) to investigate the effect of different operating parameters such as airflow rate and plate voltage on the protein and fiber enrichment level and their separation efficiencies; (2) to evaluate the fractionation performance by studying soy flour's particle size and morphology; and (3) to determine the distribution of protein and fiber particles along the negatively charged plate surface.

2. Experimental materials and methods

2.1. Materials

Commercially available soybean meal flour defatted using hexane was purchased from Honeyville (Ogden, UT, USA) and stored in a polyethylene container at −20 °C. On a dry basis, it contained 3.3 ± 0.4 wt% oil, 55.3 ± 2.1 wt% protein, 15.4 ± 0.0 wt% dietary fiber, and 6.2 ± 0.3 wt% ash. To considerably minimize the influence of humidity on the separation performance, the soybean meal flour was dried for 48 h at 103 °C before every tribo-electrostatic separation experiment. Selenium oxychloride (99%, metal basis), crystalized potassium sulfate (99.9%), and Nessler reagent were acquired from Alfa Aesar (Haverhill, MA, USA), VWR International (Radnor, PA, USA), and Ricca Chemical Company (Arlington, TX, USA), respectively. They were employed during the digestion and direct nesslerization steps of the Kjeldahl analysis. Heat-stable α-amylase solution, protease powder from Bacillus licheniformis, amyloglucosidase solution from Aspergillus niger, MES hydrate (99.5 + %), and Trizma base (99.9 + %) were purchased from Sigma-Aldrich, Inc. (St. Louis, MO, USA) and used for total dietary fiber content determinations. VWR International (Radnor, PA, USA) provided the diethyl ether, petroleum ether, ethanol, and hydrochloric acid to measure oil content in soybean meal flour and electrostatically separated fractions.

2.2. Tribo-electrostatic separation

The vertical lab-scale tribo-electrostatic separator was designed by our research team and custom-built by Ashby Manufacturing Company (Cranberry Township, PA, USA). It consisted of a fluidized bed system, a straight polytetrafluoroethylene (PTFE) tribo-charger tube, a rectangular fractionating chamber with positive and negative copper-plate electrodes connected to the high DC voltage supply apparatus (ES813 electrostatic/high voltage generator, ESDEMC Technology, Rolla, MO, USA), compressed air cylinder (Robert Oxygen Company Inc.,

Bladensburg, MD, USA) and a flowmeter (Fig. 1). The fluidized bed reservoir was cylindrical in shape with the dimensions of 15 cm in height and 10 cm in diameter, and it was made from UV-resistant polycarbonate material. An air distributor plate made from stainless steel wire mesh was located about 4 cm above the bottom of the reservoir (Fig. 1). The airflow rate was adjusted and recorded by an installed flow controller.

Approximately 45 g of soybean meal flour was first placed in the fluidized bed for each tribo-electrostatic separation. Then it was suspended into the bed vessel by introducing the compressed air at a constant flow rate through the bottom nozzle installed underneath the distributor plate. Next, the entrained soy flour particles in the airstream were pneumatically traveled towards the PTFE tribo-charger tube (3/16 in or 4.76 mm inside diameter and 150 cm in length), where they were charged through inter-particle and wall-particle collisions. The imparted surface charge values differed based on the milled particle's surface chemical composition. For example, according to Mayr and Barringer (2006) and Tabtabaei et al. (2016a), the particles rich in protein get a positive charge, whereas particles enriched by carbohydrates acquire a negative charge or no charge upon physical contact with the PTFE surface.

After tribo-charging in the tube, soy flour particles were conveyed into the fractionation chamber and eventually separated into three fractions based on their acquired charges under high voltage. Upon completing fractionation, the protein-enriched fraction designated as "NCP" was collected from the negatively charged plate, while the fiber-enriched fraction represented as "PCP" was collected from the positively charged plate. Finally, gravity attracted the weakly-charged or uncharged particles to the chamber bottom as a "CB" fraction. The resulting three fractions from each separation experiment were weighed and analyzed for their protein and dietary fiber content based on the procedures of sections 2.6 and 2.7.

The yield (%), protein separation efficiency (i.e., % of total protein), and fiber separation efficiency (i.e., % of total fiber) were measured according to each fraction's (i.e., NCP, PCP, or CB) weight, protein, and fiber content using Eqs. (1)–(3), respectively.

Yield (%) = (mass (g) of each fraction) / (mass (g) of original soybean meal flour) × 100 (Eq. 1)

Percentage of total protein (%) = (protein (g) in each fraction) / (protein (g) in original soybean meal flour) × 100 (Eq. 2)

Percentage of total fiber (%) = (fiber (g) in each fraction) / (fiber (g) in original soybean meal flour) × 100 (Eq. 3)

During each fractionation experiment, some of the soybean meal flour initially placed in the fluidized bed were lost due to adhesion on the air distribution screen in the fluidized bed and the inside surfaces of the fluidized bed and the tribo-charger tube as well as the front and back sides of the separation chamber. Therefore, the percentage of sample loss was also calculated based on Eq. (4).

Percentage of sample loss (%) = (mass (g) of original soybean meal flour – mass (g) of all collected fractions including NCP, PCP, and CB) / (mass (g) of original soybean meal flour) (Eq. 4)

The fractionation of soybean meal flour was conducted in duplicate for six different experimental conditions at two airflow rates (7 LPM and 15 LPM) and at three plate voltages (±1.0 kV, ±3.5 kV, and ±6.5 kV), as shown in Fig. 2. The airflow rate is an essential variable affecting the charging of flour particles in the tube, while plate voltage significantly affects the separation efficiency. Their overall process performance was evaluated by yield, protein/fiber content, and percentage of total protein/fiber values.

2.3. Protein and fiber distribution across the negatively charged electrode

To determine how protein and fiber particles are distributed on the negatively charged electrode plate under different airflow rates and plate voltage values, the plate was equally divided into two sections to collect two NCP fractions (i.e., NCP-T and NCP-B) from the top and bottom sections. Then, the same operating conditions were applied for the NCP-T and NCP-B protein-rich fractions, as shown in Fig. 2.

2.4. Particle size distribution

The particle size distributions of the soybean meal flour and electrostatically fractionated protein- and fiber-enriched fractions were duplicated using a Mastersizer 2000 (model APA, 2000; Malvern Instruments Ltd.) equipped with Scirocco 2000 dry dispersion unit (model ADA, 2000; Malvern Instruments Ltd.). The dispersion pressure of 1 bar was applied during particle size measurements. The volume-weighted ($D_{N4,3}$) and surface-weighted ($D_{N3,2}$) mean diameters were determined using Eqs. (5) and (6), where n_i denotes the number of particles with diameter d_i. Furthermore, the particle size diameters serving as the 10% (D_{V10}), 50% (D_{V50}), and 90% (D_{V90}) cumulative points were taken from the volume-based particle size distribution curves.

$$D_{N4,3} = \sum n_i d_i^4 \Big/ \sum n_i d_i^3 \quad \text{(Eq. 5)}$$

$$D_{N3,2} = \sum n_i d_i^3 \Big/ \sum n_i d_i^2 \quad \text{(Eq. 6)}$$

2.4.1. Scanning Electron Microscopy (SEM)

The SEM images of the soybean meal flour and its resulting protein- and fiber-rich fractions from tribo-electrostatic separation were obtained by Phenom G2 pure Scanning Electron Microscopy (Phenom-

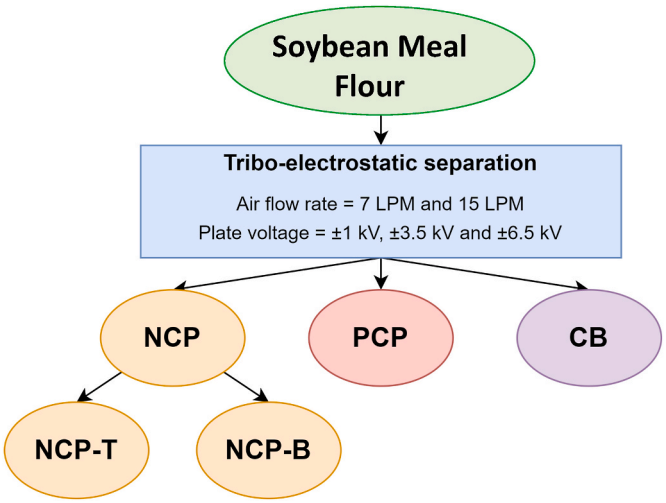

Fig. 2. Schematic representation of the tribo-electrostatic separation approach. "NCP-T" is the protein-rich fraction collected from the top half section of the negatively charged plate electrode. "NCP-B″ is the protein-rich fraction collected from the bottom half section of the negatively charged plate electrode. "PCP" is the fiber-rich fraction collected from the positively charged plate electrode. "CB" is the fraction collected from the chamber bottom.

World BV, Netherlands). All samples were initially placed onto carbon tabs (Pelco Tabs, Ted Pella Inc., Redding, CA, USA) and aluminum pin mounts (SEM Pin Stub Mount, Ted Pella Inc., Redding, CA, USA) during the SEM mounting, and pre-treated with pure gold coating. Then they were analyzed at 10 kV acceleration voltage at room temperature.

2.5. Protein content

The original soybean meal flour and all collected fractions obtained by tribo-electrostatic separation were analyzed for protein content. Crude protein composition (N × 6.25) was determined in triplicate by determination of micro-Kjeldahl nitrogen based on the procedure developed earlier (Tabtabaei et al., 2016a, 2016b) through three significant steps of acid digestion, Nesslerization, and measurement of the resultant color at 420 nm using Infinite 200 Pro Microplate Reader (Tecan Trading AG, Switzerland).

2.6. Total dietary fiber content

The total dietary fiber concentrations of original flour and all resulting electrostatically separated fractions were measured in duplicate based on the AOAC official method 991.43 (Lee et al., 1992) with some minor modifications. The method consists of sequential enzymatic digestion for protein and starch removal, enzyme digestate treatment with alcohol for the precipitation of soluble dietary fiber, washing, drying, and weighing. The weight of the initial samples and the amount of all used chemical reagents was decreased twice from the original AOAC approach, but timing, temperature, pH adjustments, stirring, and order of chemicals addition were strictly followed by the manual. The last and main modification was the replacement of vacuum filtering with the centrifugation, where the residues were centrifuged at 1000×*g* for 10 min after each mixing with 78% ethanol, 95% ethanol, and acetone. This process was repeated one more time and imitated the washing by vacuum filtration, where the desired solid constituent was separated from the unwanted liquid. The resulting values of dried fiber residue were corrected for blank, protein, and ash.

Table 1
Composition of soybean meal flour (dry-basis).

Analysis	Units	Compositions
Protein Content %	%	55.3 ± 2.1[a]
Dietary Fiber Content %	%	15.4 ± 0.0[b]
Oil Content %	%	3.3 ± 0.4[a]
Ash Content %	%	6.2 ± 0.3[b]

[a] The values represent the means (n = 3) ± standard deviation.
[b] The values represent the means (n = 2) ± standard deviation.

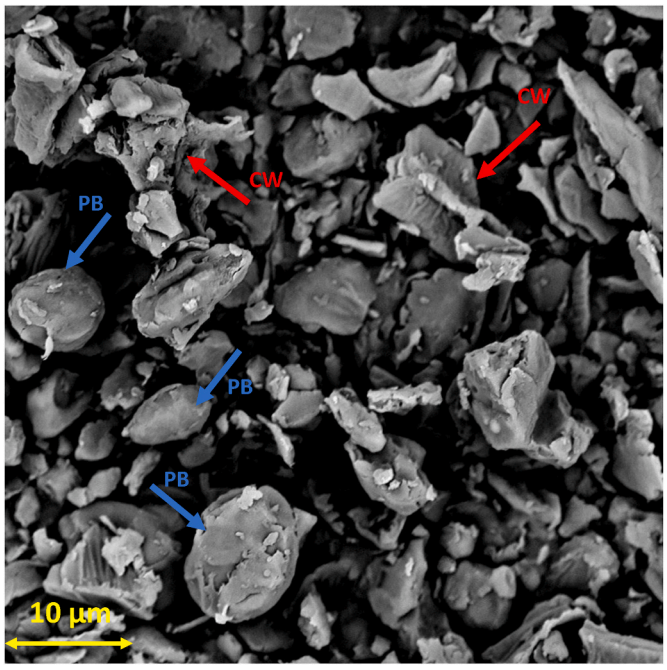

Fig. 3. Scanning Electron Microscopy (SEM) image of the soybean meal flour. CW – cell wall, PB – protein body.

2.7. Other analytical methods

The oil content of original soy flour was determined in triplicate according to the AOAC official method 922.06 (AOAC, 2016). The ash content was analyzed in duplicate based on the approved AACC method 08–01 (AACC, 2012).

2.8. Statistical analysis

To conduct pairwise t-tests on all mean averages at a 5% significance level, the SAS software (version 9.4, SAS Institute Inc., Cary, NC, USA) was used through the Least Significant Difference (LSD) analysis procedure.

3. Results and discussion

3.1. Composition and SEM of the soybean meal flour

The composition of soybean meal flour is summarized in Table 1. On a dry basis, it contained 55.3% protein, 15.4% dietary fiber, 3.3% oil, and 6.2% ash. The SEM image of soybean meal flour before electrostatic separation (Fig. 3) showed that the protein body mainly was detached from the cell walls. The protein body of soybeans is spherical in shape and 2–10 µm in diameter (Medic et al., 2014). Most of the selected soy protein bodies had an average particle size of 10 µm, which is consistent with Medic et al. (2014) study and the findings of Xing et al. (2018) on the defatted milled soy flour. Our previous study on the tribo-charging behavior of protein particles with PTFE tribo-charger tube showed that the soybean protein concentrate acquired a net positive charge, and the increasing soy protein content resulted in a higher charge value (Tabtabaei et al., 2016a).

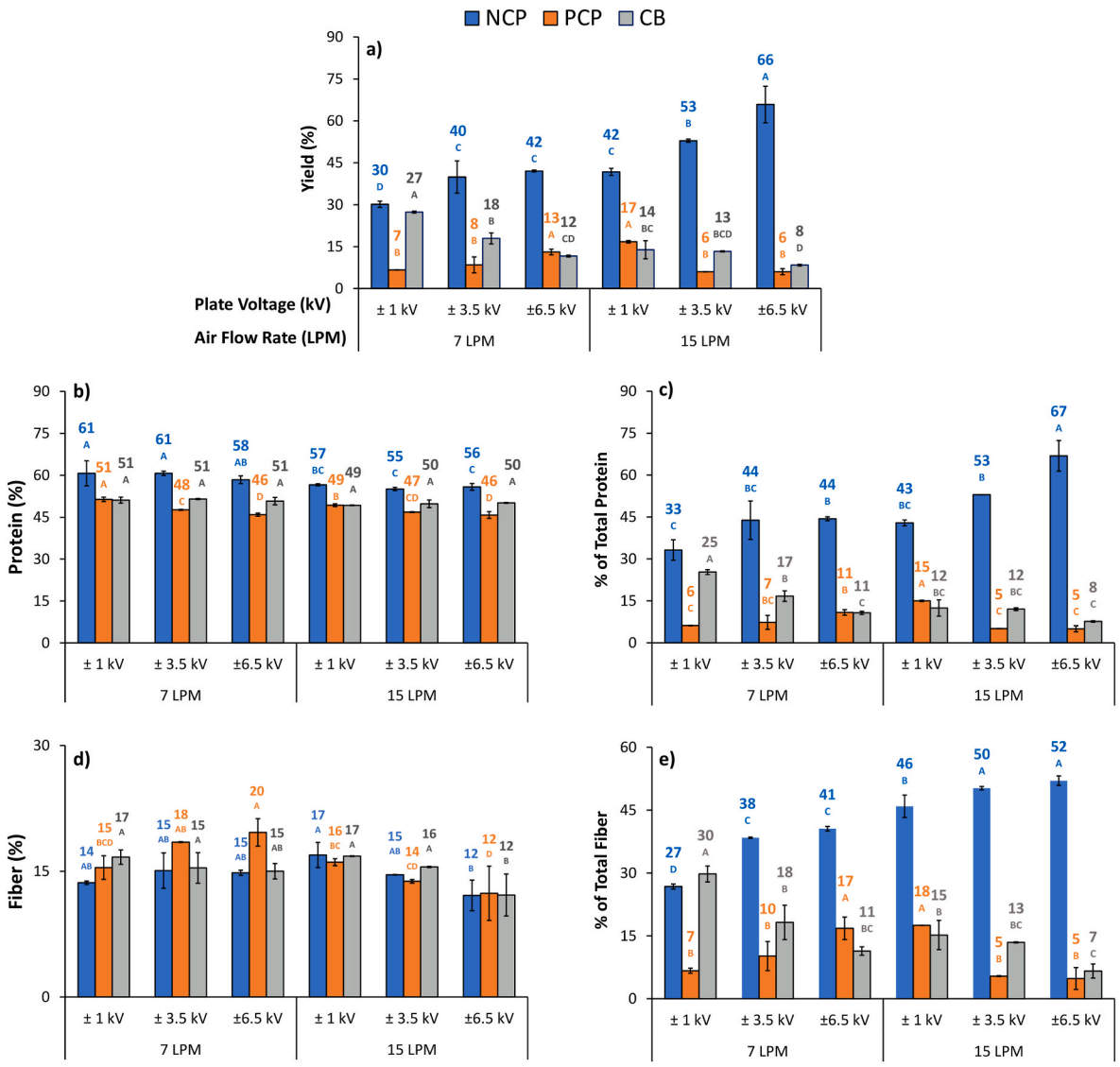

Fig. 4. a) Yield; b) protein content - dry-basis; c) protein separation efficiency; d) fiber content - dry-basis; e) fiber separation efficiency of the fractions obtained during the tribo-electrostatic separation. "NCP" is the protein-rich fraction from the negatively charged plate electrode. "PCP" is the fiber-rich fraction collected from the positively charged plate electrode. "CB" is the fraction collected from the chamber bottom. The protein and fiber content (dry basis) of the starting soybean meal flour was 55.3 and 15.4%, respectively (Table 1). ^{ABC} Yields, protein content, fiber content and percentages of total protein and fiber in each electrostatically separated fraction obtained at all tested plate voltages and airflow rates with different upper-case letters are significantly different ($P < 0.05$). Percentage of sample loss (Eq. (4)) at laminar air flow rate (7 LPM) was calculated as 35.8 ± 1.5, 33.7 ± 0.9, and 33.3 ± 1.0% at ±1, ±3.5, and ±6.5 kV, respectively. Percentage of sample loss (Eq. (4)) at turbulent air flow rate (15 LPM) was calculated as 27.6 ± 1.5, 27.8 ± 0.7, and 19.8 ± 5.2% at ±1, ±3.5, and ±6.5 kV, respectively.

3.2. Effects of airflow rates and plate voltages on protein and fiber separation efficiency

The soybean meal flour went through a tribo-electrostatic separation, and its performance was evaluated at different airflow rates and plate voltages in terms of yield, protein content, fiber content, and percentages of total protein and fiber from three collected fractions (NCP, PCP, and CB) as shown in Fig. 4. Both operating conditions of airflow rate and plate voltage had a notable influence on the yield and protein and fiber enrichment levels (Fig. 4). Similar to our previous studies on navy bean flour (Tabtabaei et al., 2016b) and sieved oat groats (Konakbayeva et al., 2022; Konakbayeva and Tabtabaei, 2021), the protein-rich fraction (NCP) was collected from the negatively charged electrode plate, while fiber-enriched fractions (PCP) were collected from the positively charged plate.

The NCP fraction had the highest yield in all experiments, and it was increased with the increasing value of both airflow rate and plate voltage, as shown in Fig. 4a. Hence, most of the flour entering the separation chamber was attached to the negatively charged electrode plate. The NCP fractions obtained at an airflow rate of 15 LPM had much higher yields than those collected at the airflow rate of 7 LPM. The NCP fraction obtained at 15 LPM and the maximum tested plate voltage of ±6.5 kV had the highest yield of 65.9%, compared to 42.0% for the NCP fraction at 7 LPM and ±6.5 kV (Fig. 4a). This is attributed to the shift of airflow pattern in the tribo-charging tube from laminar to turbulent when the airflow rate was changed from 7 LPM (Re = 1992) to 15 LPM (Re = 4266), respectively. A similar trend was noticed in the protein separation efficiency of the NCP fractions obtained at 15 LPM (Fig. 4c). This is consistent with our previous study on the protein enrichment for the navy bean flour, which showed significantly higher yield values for the protein-rich fractions obtained at the turbulent airflow rate of 9 LPM (Tabtabaei et al., 2017b).

Furthermore, the electrode plates started to attach more positively charged particles with rising plate voltages under both flows, thus lifting

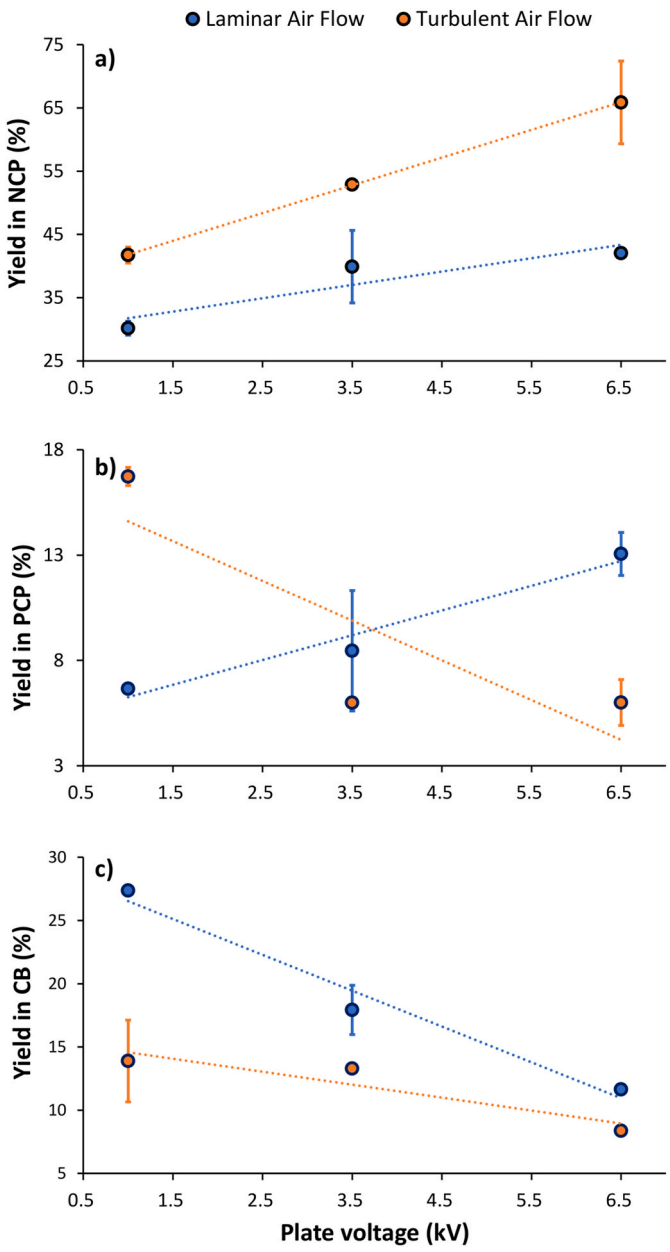

Fig. 5. Influence of plate voltage on the yield of the fractions collected during the tribo-electrostatic separation at laminar and turbulent airflow rates. "NCP" is the protein-rich fraction from the negatively charged plate electrode. "PCP" is the fiber-rich fraction collected from the positively charged plate electrode. "CB" is the fraction collected from the chamber bottom. The lines were only added for visual guidance.

the yield of NCP fractions at both laminar (7 LPM) and turbulent (15 LPM) conditions. By increasing the plate voltage from ±1 to ±6.5 kV, the yield of the PCP fraction was almost doubled (from 7 to 13%) at the laminar airflow rate, while its yield was significantly ($P < 0.05$) reduced (from 17 to 6%) at the turbulent condition (Fig. 4a). On the other hand, the yield of the CB fractions was decreased at both airflow rates by increasing the plate voltage values, representing that at higher plate voltages, fewer particles are directed to the bottom of the separator by gravity. This clearly confirms that particles charged under turbulent flow are mostly deflected towards the negatively charged plate, reducing the yields of the CB and PCP fractions.

The maximum obtained protein content for the NCP fraction at the laminar and turbulent airflow rates was 60.7 and 56.6% (Fig. 4b), respectively, which accounted for 5.4 and 1.3% protein enrichment of the starting material (i.e., 55.3%). Similar maximum protein beneficiation between 3.7 and 6.5% was obtained for two types of soybean meal flours prepared by oil pressing or defatted by petroleum ether as organic solvent (Xing et al., 2018). Other oilseeds such as milled lupine flour and rapeseed oil cake (cold pressed and dried) were enriched by 16.8% (Wang et al., 2016) and 10% (Basset et al., 2016) more protein after one-step tribo-electrostatic separation, respectively. The tribo-electrification at 7 LPM demonstrated the ability to enrich the original soy flour protein to a relatively high value. The lower protein content at 15 LPM might be due to the overcharging of particles by the turbulent flow that resulted in agglomerates formation and poor dispersibility of protein and dietary fiber particles (Tabtabaei et al., 2017b; Wang et al., 2015a). The negatively charged plate can attract such agglomerates with a net positive charge, and it explains the increase in yield and protein separation efficiency, also the decrease of the protein content of the NCP fraction at a higher airflow rate.

It should be noted that all NCP fractions had higher protein purity compared to the starting soybean meal flour (i.e., 55.3%) except for the separation performed at 15 LPM and ±3.5 kV, while all PCP fractions had depleted protein content. All CB fractions almost stayed the same in protein content (~49–51%) throughout the experiments, and their protein content values were lower than the protein content of the starting material (i.e., 55.3%). The protein content of the NCP fraction was slightly ($P < 0.05$) decreased by increasing plate voltage at both laminar and turbulent airflow rates, and it contradicted our expectation since stronger electric field strength was assumed to attract more protein-rich particles. As can be seen in Fig. 4b, at laminar airflow rate, the protein content of the NCP fraction was reduced from 61 to 58% by increasing the plate voltage from ±1 to ±6.5 kV. The same trend was observed for the protein content of the NCP fraction at the turbulent air flow rate (15 LPM), where its protein content was reduced from 57% at low plate voltage of ±1 kV to 55 and 56% (statistically similar, $P < 0.05$) at higher plate voltages of ±3.5 and ± 6.5 kV. However, the considerable increase in the yield and protein recovery of the NCP fractions at higher plate voltages may have resulted in electrode fouling. Such shielding can reduce the electric field strength (Cangialosi et al., 2008; Tabtabaei et al., 2017b), thus slightly decreasing the protein content of the NCP fractions. Therefore, significant protein enrichment was obtained at the lower plate voltages of ±1 to ±3.5 kV and lower airflow rate (7 LPM).

The highest fiber content of 19.6% was obtained at laminar flow and ±6.5 kV for the PCP fraction (Fig. 4d), which enriched the fiber of the starting soy flour (i.e., 15.4%) by 4.2%. The fiber enrichment of soybean meal was less than the rapeseed oil cake (cold pressed and dried) observed by Basset et al. (2016) after single-step tribo-electrostatic separation (11% lignin enrichment). Some fiber particles have also been recovered in the NCP fraction. The possible explanation for this might be the manufacturer's too fine milling of the flour, which led to the particles clustering with an overall positive charge. The fiber content and its recovery were mainly higher in CB than PCP fraction, which might be due to fiber's lower chargeability than the protein. The protein-enriched NCP fraction had higher protein purity and lower fiber purity than that of the PCP fraction at the laminar airflow rate (Fig. 4b and d). The yield, fiber content, and fiber separation efficiency of fiber-enriched PCP fraction were increased by plate voltage at constant laminar flow, but the reverse tendency was observed for the turbulent flow, as shown in Fig. 4a, d-e. The reason might be attributed to the migration of too fine negatively charged fibers and carbohydrates to the negatively charged plate since they are more affected by the transporting gas than the electrostatic force (Xing et al., 2018). Such a phenomenon can also explain the decrease in the protein of the PCP at a higher airflow rate (Fig. 4b). Hence, an improved fiber enrichment was noted at the laminar flow (7 LPM) and higher separation voltage (±6.5 kV).

The effect of plate voltage on the yield of three fractions is represented in Fig. 5. During the separation at ±6.5 kV and turbulent flow, 65.9% of the initial flour was deposited on the negatively charged plate

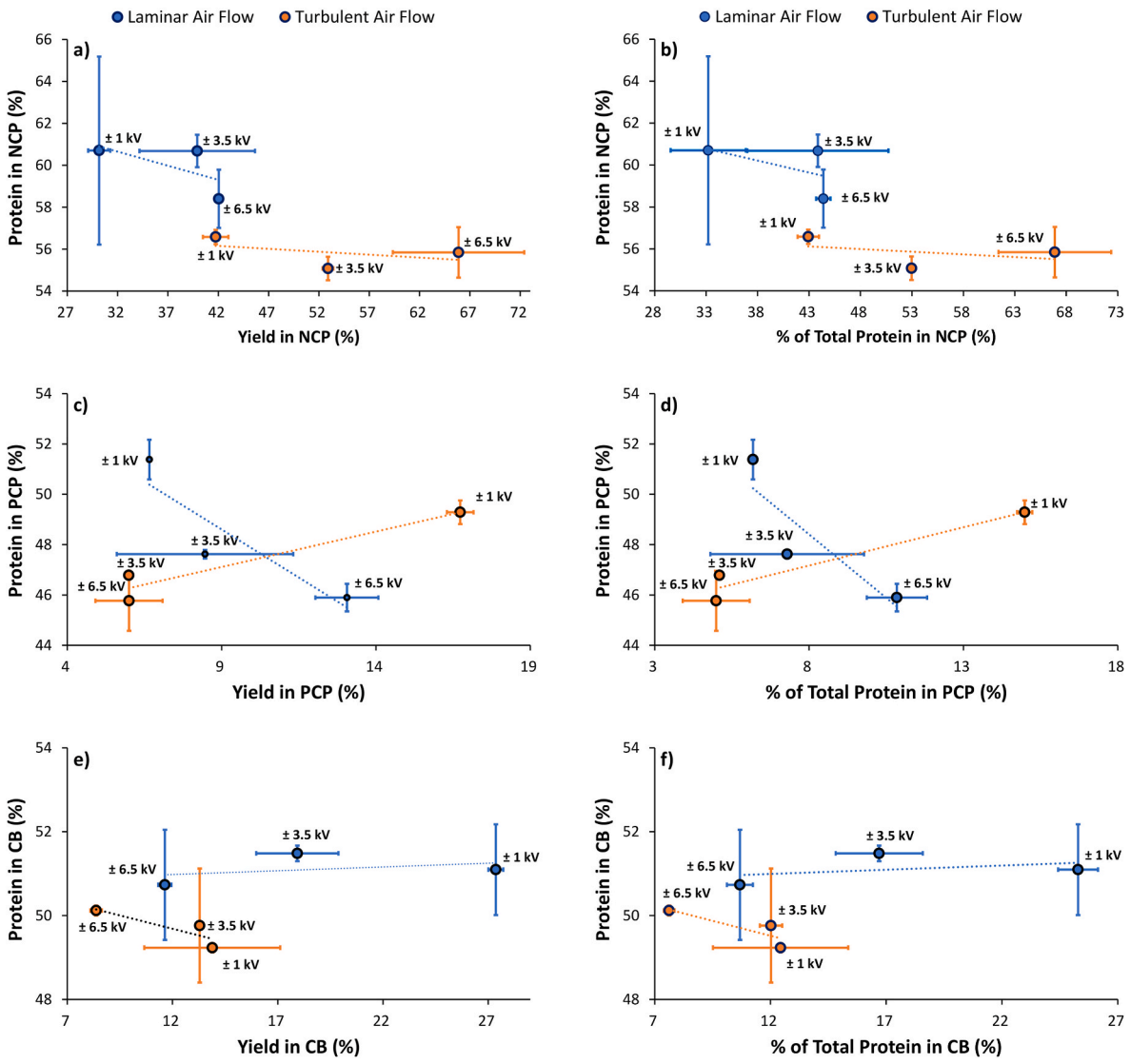

Fig. 6. Protein content as a function of yield and protein separation efficiency for the fractions collected during the tribo-electrostatic separation at laminar and turbulent airflow rates. "NCP" is the protein-rich fraction from the negatively charged plate electrode. "PCP" is the fiber-rich fraction collected from the positively charged plate electrode. "CB" is the fraction collected from the chamber bottom. The lines were only added for visual guidance.

(Fig. 5a), while only 6.0 and 8.4% were attracted to the positively charged plate and chamber bottom (Fig. 5b–c), respectively. The yields of the PCP fractions increased with plate voltage at laminar flow but decreased significantly at turbulent airflow rate. However, the yields of the CB fractions fell moderately at both laminar and turbulent airflow rates. However, the decreasing trend of PCP yield by plate voltage (Fig. 5b) is more notable than the neutral CB (Fig. 5c) at turbulent flow, meaning most soy flour particles were positively charged.

The relationship between the protein content of three fractions (NCP, PCP, and CB) and their corresponding yield and percentage of total protein are presented in Fig. 6. Both yield and protein separation efficiency showed similar behavior according to the protein content of the NCP (Fig. 6a–b), PCP (Fig. 6c–d), and CB (Fig. 6e–f) fractions. Fig. 6a–b shows that the better result for the protein content of NCP fraction was achieved at lower airflow rate and separation voltage values, whereas the better performance for the yield and protein recovery was observed at higher airflow rates and separation voltages. The previous study on the starch-rich legume flour of navy bean flour also revealed the exact influence of separation parameters on protein-rich fractions' protein content and protein separation efficiency (Tabtabaei et al., 2016b). Changing the plate voltage from ±1.0 kV to ±3.5 kV improved the yield of the NCP fraction without compromising its protein content at a laminar flow rate (Fig. 6a).

The NCP fraction's slightly reduced protein enrichment level was observed at higher yields (Fig. 6a) and protein separation efficiencies (Fig. 6b) at laminar and turbulent airflow rates. The highest level of protein depletion in the PCP fraction was observed at the high voltage of ±6.5 kV and turbulent flow, where the lowest yield (~6%) and protein separation efficiencies (~5%) were obtained. At the laminar flow, the highest level of PCP's protein depletion was observed at ±6.5 kV with a relatively high yield (~13%) and protein separation efficiency (~11%). The CB's protein content seems independent of yield and protein separation efficiency at the laminar condition.

The relationships between fiber content and yield as well as fiber content and fiber separation efficiency, were evaluated individually for three fractions in Fig. 7. As in Fig. 6, the same behavior was observed for the yield and fiber recovery for all NCP, PCP, and CB fractions, except for the turbulent flow values of the NCP fraction (Fig. 7 a-b). A substantial change towards better fiber purity, yield, and fiber recovery was achieved at laminar air flow rate and higher plate voltage value for the desired PCP fraction, apart from one outlier at ±1.0 kV of turbulent flow with the highest yield (Fig. 7 c-d). While the PCP's fiber content

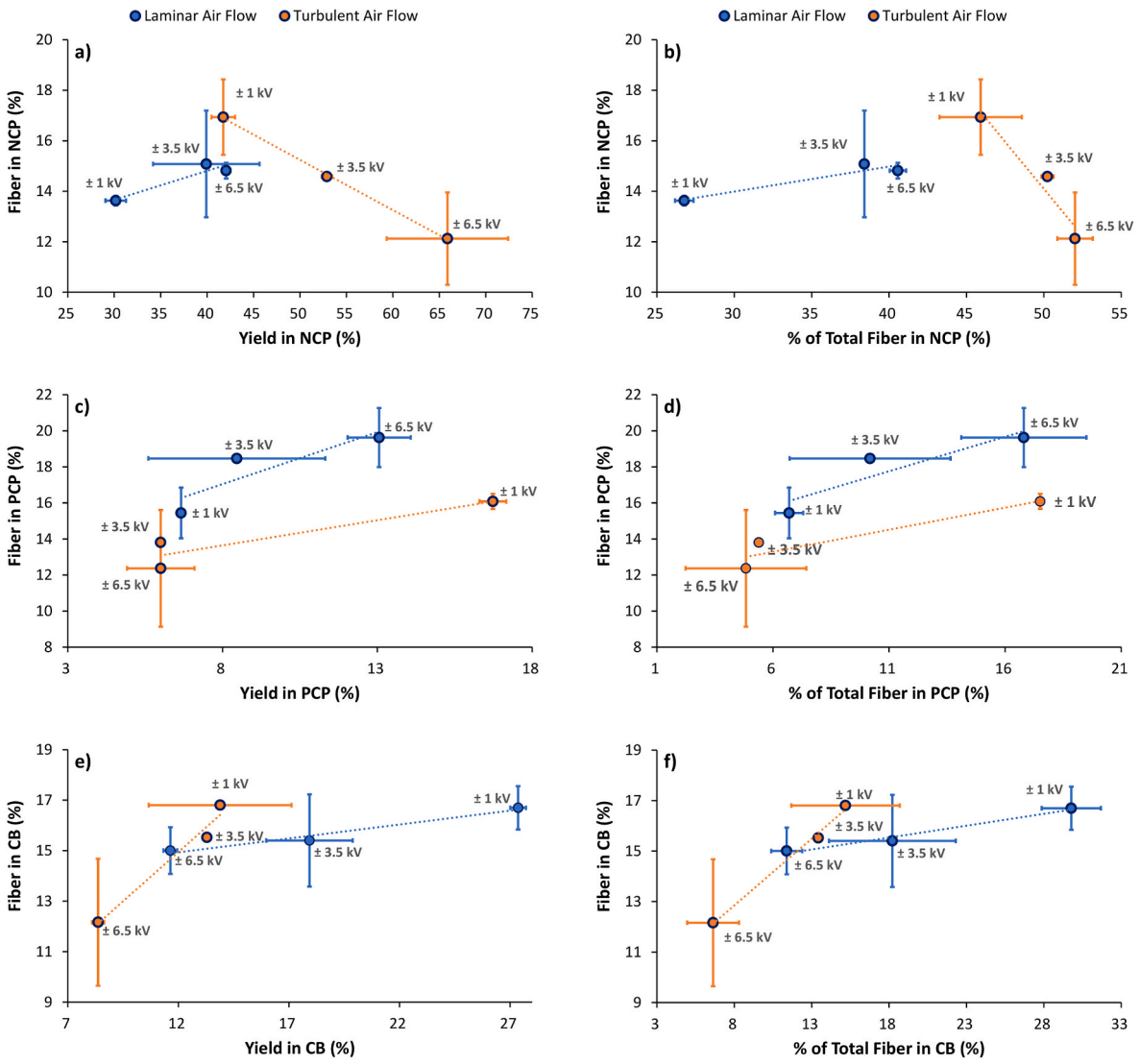

Fig. 7. Fiber content as a function of yield and fiber separation efficiency for the fractions obtained during the tribo-electrostatic separation at laminar and turbulent airflow rates. "NCP" is the protein-rich fraction from the negatively charged plate electrode. "PCP" is the fiber-rich fraction collected from the positively charged plate electrode. "CB" is the fraction collected from the chamber bottom. The lines were only added for visual guidance.

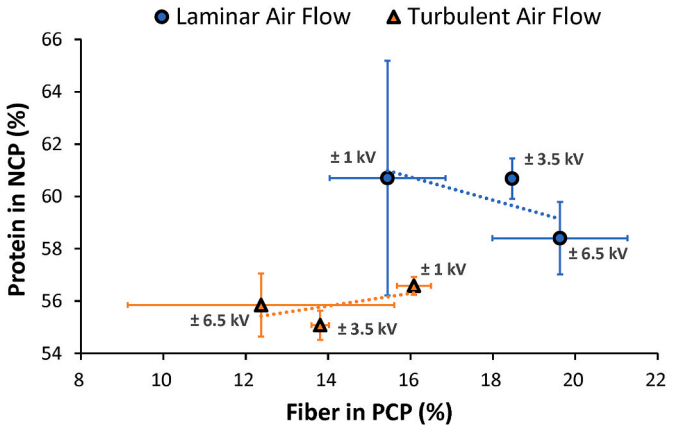

Fig. 8. Protein content of the fraction collected from the negatively charged plate (NCP) as a function of fiber content of the fraction collected from the positively charged plate (PCP). The lines were only added for visual guidance.

Table 2
Sample loss percentages during tribo-electrostatic separations.

Tribo-electrostatic separation (TES) conditions		Sample loss[a] (%)
Air flow rate *(LPM)*	Plate voltage *(kV)*	
7	±1	35.8 ± 1.5^{A}
	±3.5	33.7 ± 0.9^{A}
	±6.5	33.3 ± 1.0^{A}
15	±1	27.6 ± 1.5^{B}
	±3.5	27.8 ± 0.7^{B}
	±6.5	19.8 ± 5.2^{C}

^{ABC} Means sharing the same capital superscripts in each column are not significantly different ($P < 0.05$).

[a] Sample loss was calculated using Eq. (4). The values represent the means ($n = 2$) ± standard deviation.

obtained at 7 LPM improved with the increasing voltage, experiments performed at 15 LPM provided elevated values with the decreasing voltage (Fig. 7 c-d).

The highest depletion of fiber content in the NCP (Fig. 7a–b) fraction was observed at turbulent flow and plate voltage of ±6.5 kV with a high yield of 65.9% and fiber efficiency of 52.0%. The highest depletion of

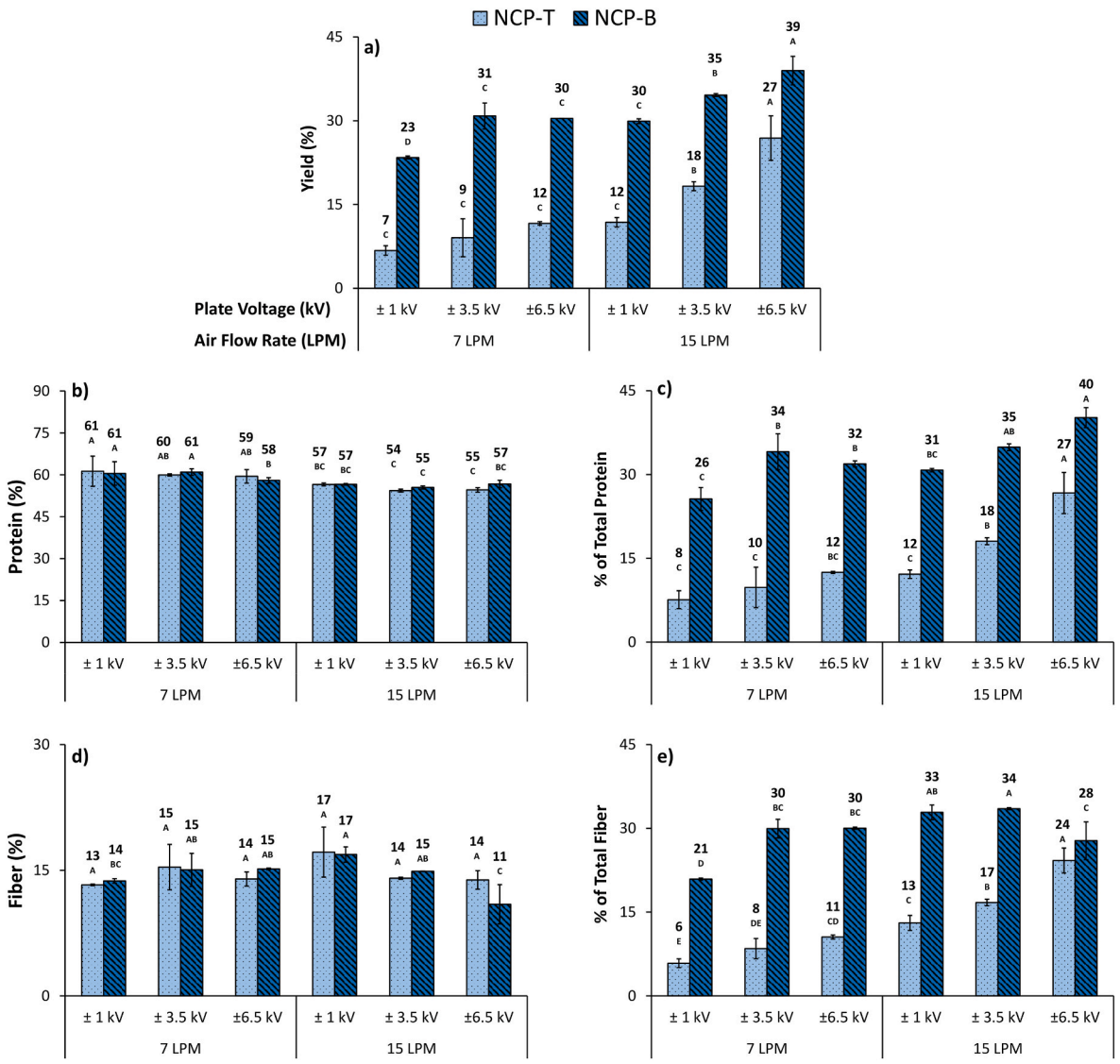

Fig. 9. a) Yield; b) protein content – dry basis; c) protein separation efficiency; d) fiber content – dry basis; e) fiber separation efficiency of NCP-T and NCP-B fractions obtained during the tribo-electrostatic separation. "NCP-T" is the protein-rich fraction collected from the top half section of the negatively charged plate electrode. "NCP-B" is the protein-rich fraction collected from the bottom half section of the negatively charged plate electrode. [ABC] Yields, protein content, fiber content and percentages of total protein and fiber in each protein-rich fraction obtained at all tested plate voltages and airflow rates with different upper-case letters.

fiber content in the CB (Fig. 7e–f) fraction was observed at turbulent flow and plate voltage of ±6.5 kV, where the lowest yield (~8%) and fiber separation efficiency (~7%) was obtained.

The protein content of the NCP fractions as a function of fiber content in the PCP fractions are shown in Fig. 8. Both NCP and PCP fractions experience their higher protein and fiber contents, respectively, at laminar air flow rate. The fiber content in the PCP increases significantly as the protein content reduce for NCP fractions at the laminar airflow rate. The lower airflow rates and plate voltages (±1 to ±3.5 kV) resulted in better protein content for protein-enriched NCP fraction, while the lower airflow rate and higher plate voltage show higher fiber for the fiber-enriched PCP fraction (Fig. 8). Both target fractions have their best scenario with the laminar flow, but their plate voltages of better experiment settings do not meet each other, and hence the best voltage condition should be chosen. In Fig. 5a–b, the NCP and PCP fragments had yields increasing with the higher value of plate voltage at laminar flow, and therefore ±6.5 kV is found to suffice both fractions.

Concluding, among different combinations of airflow rates and plate voltages, 7 LPM with ±6.5 kV resulted in the highest yield of particles with modest protein and fiber enrichment. With tribo-electrostatic separation, the protein content of the original soybean meal flour was increased from 55.3% to 58.4%, while the fiber content was improved from 15.4% to 19.6% at a laminar airflow rate of 7 LPM and plate voltage of ±6.5 kV. This resulted in 44.4% of total available protein and 16.8% of the total available fiber in the NCP and PCP fractions, respectively.

The sample loss percentages during tribo-electrostatic separations at all tested airflow rates and plate voltages are included in Table 2. As can be seen, the percentages of sample loss at laminar air flow rate remain statistically constant ($P < 0.05$) around 34.3% (average of 35.8, 33.7, and 33.3% at different palate voltages), indicating that plate voltage cannot significantly affect the sample loss at laminar flow. However, the sample loss percentages were reduced significantly to ~27% at ±1 and ± 3.5 kV and 19.8% at ±6.5 kV under turbulent air flow rate. This might indicate the reduced entrapment of fluidized particles in the fluidized bed and the tribo-charger tube at the turbulent air flow rate, while higher plate voltage combined with a higher flow rate might increase the attachment of the charged particle to the electrode plates rather than the front and back sides of the fractionation chamber. Loss of samples during the tribo-electrostatic separation process reduced the yields as well as

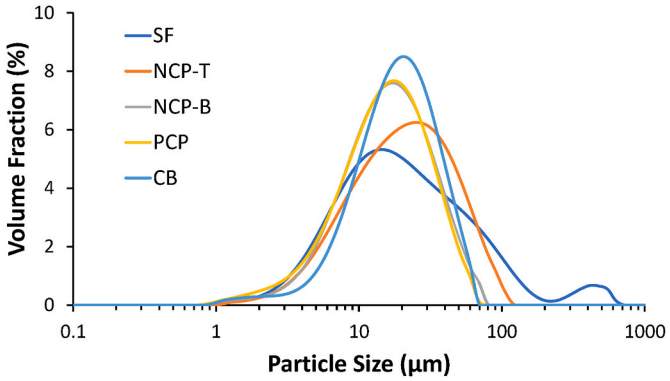

Fig. 10. Particle size distribution plots of the soybean meal flour and the fractions obtained during the tribo-electrostatic separation at7 LPM and ±6.5 kV. SF is the original soybean meal flour. "NCP-T″ is the protein-rich fraction collected from the top half section of the negatively charged plate electrode. "NCP-B″ is the protein-rich fraction collected from the bottom half section of the negatively charged plate electrode. "PCP" is the fiber-rich fraction collected from the positively charged plate electrode. "CB" is the fraction collected from the chamber bottom.

protein and fiber separation efficiencies of the NCP, PCP, and CB fractions. The lower the losses, the higher the yields and, eventually, protein and fiber separation efficiencies.

3.3. Analysis of protein and fiber distribution across the negatively charged electrode plate at different airflow rates and plate voltages

The negatively charged plate was divided equally into two parts to understand the effect of airflow rates and plate voltages on the protein and fiber particles distribution. Therefore, two fractions of NCP-T and NCP-B were collected from the top and bottom sections of the plate and were evaluated for their yield, protein content, fiber content, and percentages of total protein and fiber at different operating conditions (Fig. 9a–e). At every tested airflow rate and plate voltage, the protein and fiber contents (Fig. 9b and d) of the NCP-T and NCP-B fractions were almost similar to each other, while the yield (Fig. 9a) and separation efficiencies (Fig. 9c and e) were notably higher in the NCP-B fraction collected from the bottom section of the plate compared to the NCP-T fraction deposited on the top part. A larger applied electric field (±6.5 kV) and turbulent air flow rate (15 LPM) slightly increased ($P < 0.05$) the difference between the two fractions' protein content (Fig. 9b) and significantly increased ($P < 0.05$) the difference between the two fractions' fiber contents (Fig. 9d). The airflow rate transition from laminar to turbulent led to decreased protein purity (Fig. 9b). For instance, under the same applied electric field (±3.5 kV), the protein content of the NCP-T and NCP-B fractions reduced from 60.0 and 61.0% to 54.3 and 55.5%, respectively. This corresponds with our earlier study on the navy bean flour, where protein-enriched fractions collected from the top, middle and bottom sections (PF3, PF2, and PF1, respectively) of the negatively charged electrode demonstrated lower protein content at the turbulent flow (Tabtabaei et al., 2017b). Consequently, the experiments conducted at 15 LPM could not enrich the protein content efficiently despite the voltage.

The considerable variation in the yield and separation efficiencies between NCP-T and NCP-B fractions can be explained by the high particle velocity at the chamber entrance, which slows down moving away from the separator entrance. Consequently, the bottom part of the plate has more time to catch the charged particles. The higher difference in yield and separation efficiencies of protein-rich fractions was observed during the separations performed under the laminar flow rate. For instance, at 7 LPM and ±3.5 kV, the NCP-B fraction had about 30.9% yield, 34.1% protein recovery, and 29.9% fiber recovery, which was considerably higher than the NCP-T fraction (9.0%, 9.8%, and 8.5%,

Table 3
Particle size measurements of the soybean meal flour and the fractions obtained during the optimized tribo-electrostatic separation (7 LPM and ±6.5 kV).

Fractions[a]	D_{V10} (μm)	D_{V50} (μm)	D_{V90} (μm)	$D_{N4,3}$ (μm)	$D_{N3,2}$ (μm)
Soybean Meal Flour	5.3 ± 0.0^{D}	17.6 ± 0.2^{B}	76.6 ± 1.1^{A}	20.7 ± 0.1^{B}	10.5 ± 0.1^{B}
NCP-T	5.9 ± 0.0^{B}	19.2 ± 0.0^{A}	51.3 ± 0.0^{B}	22.5 ± 0.0^{A}	12.2 ± 0.0^{A}
NCP-B	5.7 ± 0.0^{C}	15.1 ± 0.0^{C}	35.7 ± 0.1^{D}	17.2 ± 0.0^{D}	10.5 ± 0.1^{B}
PCP	5.1 ± 0.0^{E}	14.6 ± 0.1^{D}	33.3 ± 0.2^{E}	16.6 ± 0.1^{E}	9.6 ± 0.1^{C}
CB	7.0 ± 0.1^{A}	17.5 ± 0.1^{B}	37.0 ± 0.1^{C}	19.2 ± 0.1^{C}	12.0 ± 0.1^{A}

[ABC] Means sharing the same capital superscripts in each column are not significantly different ($P < 0.05$).

[a] "NCP-T" represented the fraction collected from the top of the negatively charged plate; "NCP-B″ represented the fraction collected from the bottom of the negatively charged plate; "PCP" represented the fraction collected from the positively charged plate; and "CB" represented the fraction collected from the bottom of the separation chamber.

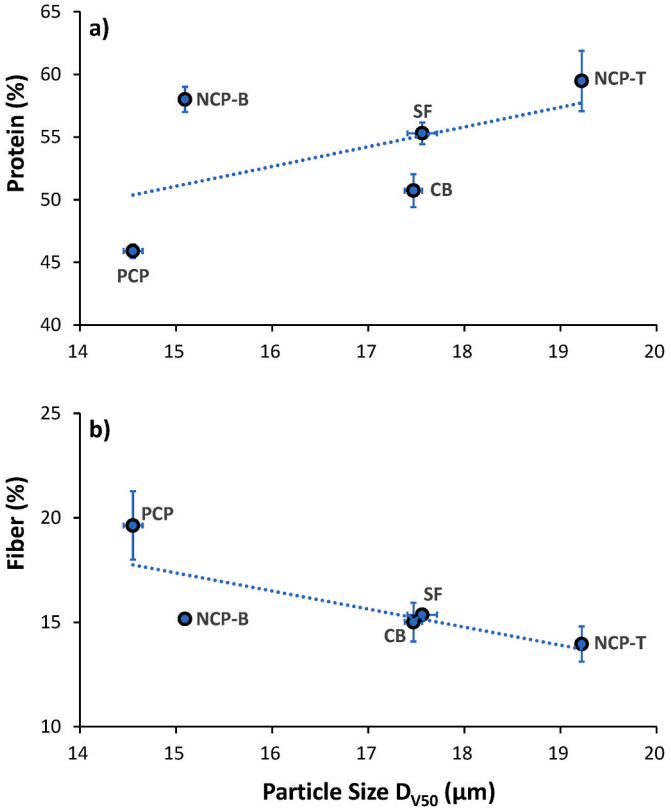

Fig. 11. Average particle size (D_{V50}) as a function of protein content and fiber content for the fractions obtained during the tribo-electrostatic separation at 7 LPM and ±6.5 kV. SF is the original soy flour. "NCP-T" is the protein-rich fraction collected from the top half section of the negatively charged plate electrode. "NCP-B″ is the protein-rich fraction collected from the bottom half section of the negatively charged plate electrode. "PCP" is the fiber-rich fraction collected from the positively charged plate electrode. "CB" is the fraction collected from the chamber bottom. The lines were only added for visual guidance.

respectively) (Fig. 9a, c, and e). The same behavior was noticed for other plate voltages (±1.0 kV and ±6.5 kV) at laminar airflow. In fact, as was discussed before, at a higher airflow rate, the flour particles should have had a higher velocity at the entrance than the separations performed at

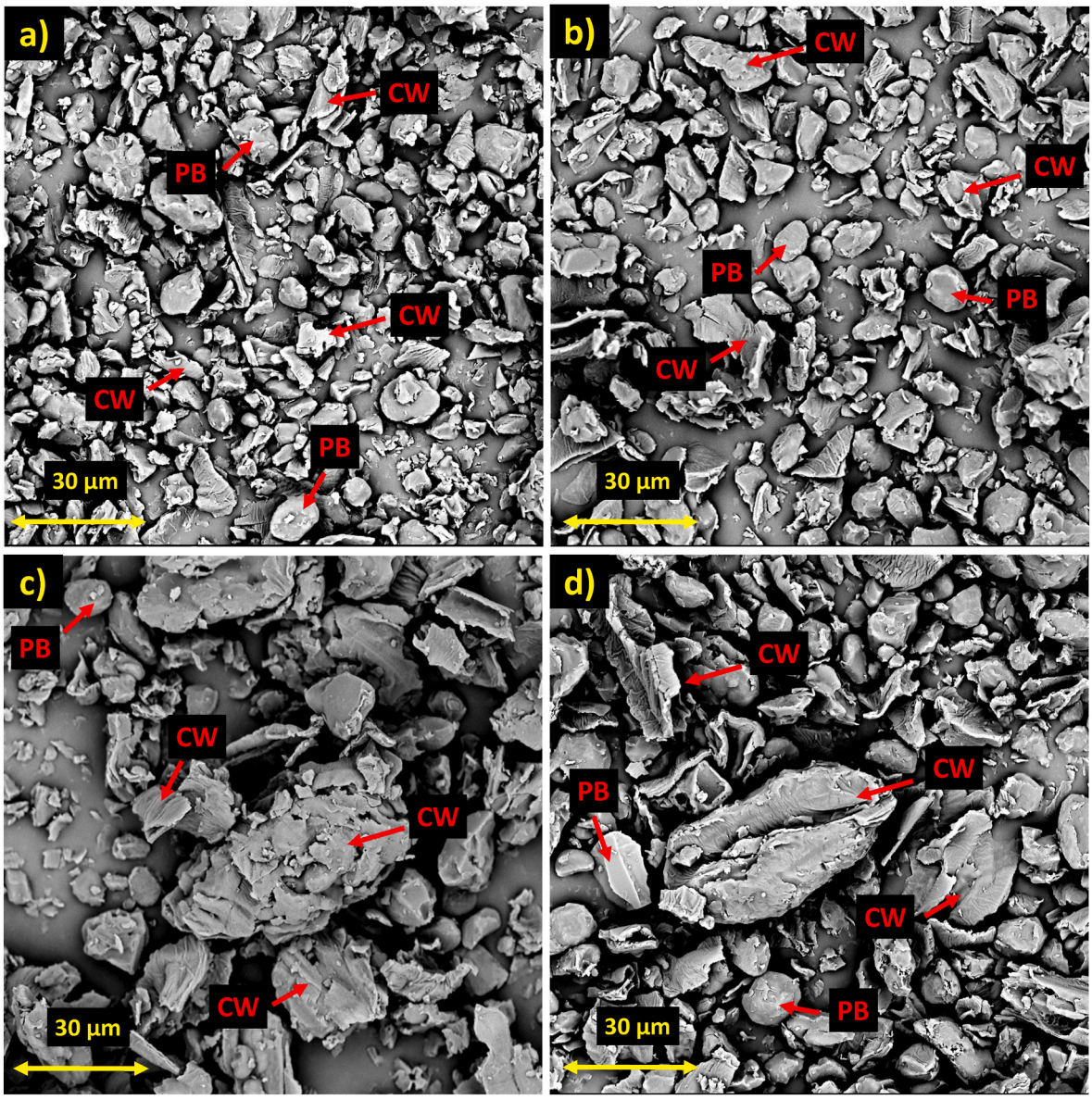

Fig. 12. SEM images of fractions obtained during the tribo-electrostatic separation at 7 LPM and ±6.5 kV: (a) "NCP-T" – protein-rich fraction collected from the top half section of the negatively charged plate electrode, (b) NCP-B – protein-rich fraction collected from the bottom half section of the negatively charged plate electrode, (c) PCP – fiber-rich fraction collected from the positively charged plate electrode, and (d) CB – fraction collected from the chamber bottom. In all SEM images, CW is acronym of cell wall and PB is acronym of protein body.

laminar flow, thus increasing the difference even more between the two sections. However, we can see that yield and recovery values increased for the NCP-T at 15 LPM. This may be caused by the higher friction in the tube at a turbulent airflow rate which provides more significant charges to the particles, and in that way, the top section of the electrode can better attract the overcharged particles. As a result, at the turbulent flow and high electric field strength (±6.5 kV), the highest yield and recovery results for the NCP-T fraction were achieved. Switching the plate voltage from ±1 to ±3.5 kV had a more significant effect on the yield and recovery values of NCP-B fractions, except for the fiber recovery at the turbulent flow rate, while the yield and recovery values of NCP-T fractions changed more slowly with the voltage change from ±1 to ±3.5 kV (Fig. 9a, c, and e). The NCP-T and NCP-B fractions at the turbulent condition and high electric field strength of ±6.5 kV had relatively close fiber separation efficiencies of 24 and 28%, respectively.

3.4. Particle size and Scanning Electron Microscopy (SEM) images of tribo-electrostatically-separated fractions

The fractions obtained at a laminar flow rate of 7 LPM and plate voltage of ±6.5 kV, were further discussed regarding their particle sizes and microstructure. Fig. 10 represents the particle size distribution curves of the NCP-T, NCP-B, PCP, and CB fractions compared to the starting soybean meal flour. It can be noticed that the NCP-T fraction's peak is located at a coarser particle size, while NCP-B and PCP fractions had coincident peaks in the same size range. The particle size analysis (Fig. 10) shows that the coarse particles (i.e., larger than ~120 µm) presented in the original soybean meal flour were technically trapped inside the fluidized bed and/or tribo-charger tube during the fractionation process at laminar flow (% of sample loss in Table 2). This can be explained by the dominant gravitational force on the large particles than the upward force influence created by the laminar airflow in the bed.

As shown in Table 3, the NCP-T fraction had the largest average

particle diameter (D_{v50}) compared to the starting soybean meal flour and other fractions collected under 7 LPM and ±6.5 kV. Both NCP-T and NCP-B fractions had, respectively, larger D_{V50} of 19.2 and 15.1 μm than the PCP fraction (D_{V50} of 14.6 μm). This observation contradicted our expectation since the navy bean protein-rich fraction produced during our previous study (Tabtabaei et al., 2019) was smaller in particle size than the starch-rich fraction. Moreover, in another tribo-electrostatic separation study by Xing et al. (2018), the protein content of soy flour increased with the reducing average particle size after the defatting and milling processes. Furthermore, the protein-rich fraction of the rapeseed meal after single-step tribo-electrostatic separation had a considerably smaller particle size than the lignin-rich fraction (D_{V50} of 74.7 and 114.6 μm, respectively) (Basset et al., 2016). In our case, the smaller particle size of the PCP fraction compared to the other electrostatically collected fractions may be attributed to the manufacturer's intensive milling of the original soybean meal flour, which led to too finely milled dietary fiber particles. This can also be explained by fine cell wall particles in the SEM image in Fig. 3, where most have similar or tinier sizes than the protein bodies. Moreover, our feed flour's initial average particle size was significantly low (D_{V50} of 17.6 μm) compared to similar studies. This can be compared with D_{V50} of 48.8 μm for starting milled soybean flour (Xing et al., 2018), D_{V50} of 126.0 μm for the starting lupine flour (Wang et al., 2016), D_{V50} of 89.7 μm for rapeseed oil cake flour (Basset et al., 2016), and D_{V50} of 48.0 μm for our previously studied pin-milled navy bean flour (Tabtabaei et al., 2017b). The interactions between smaller particles might cause more clustering due to the van der Waals force (Wang et al., 2016).

Due to the intense milling of starting soybean meal flour, the particle size distribution curves of the NCP-T, NCP-B, PCP, and CB fractions (Fig. 10) showed their peaks at sizes relatively close to each other (26.3, 17.4, 17.4, and 20.0 μm, respectively). The average particle size of the CB fraction (D_{V50} of 17.5 μm) was almost equivalent to the original flour (Table 3).

The relationship of protein and fiber content with the average particle size of the fractions was examined, and its outcome is shown in Fig. 11. The relatively close D_{v50} of soybean meal flour (i.e., 17.6 μm) to individual protein body size (~10 μm, Section 3.1 and Fig. 3) indicates the presence of fine fibers in the flour. These finely milled fiber particles were collected on the positive electrode, thus producing a fiber-enriched PCP fraction with the tiniest particle size (Fig. 11b). The NCP-T section had the most significant portion of large particles in the range of 40–120 μm (Fig. 10), which might be attributed to the agglomerates or the small group of particles in the starting flour with several protein bodies still enclosed in the cotyledon cell. Such positively and highly charged large proteinaceous particles may deposit onto the top part of the negatively charged electrode, which had a high-strength electric field (±6.5 kV). Other protein-fiber agglomerates with a relatively lower net positive charge may move down further the negative plate to be attracted by the NCP-B fraction at the lower part of the electrode. This can explain the notably high particle size difference between two protein-rich fractions of NCP-T (D_{V50} = 19.2 and $D_{N3,2}$ = 12.2 μm) and NCP-B (D_{V50} = 15.1 and $D_{N3,2}$ = 10.5 μm) across the negatively charged plate although they had similar protein and fiber content (Fig. 11). The equivalent amount of charged proteins and fibers in clusters might neutralize each other hence producing the clusters with a zero net charge (Wang et al., 2015a) which then can be attracted to the CB by gravity. The CB and starting soy flour showed similar average particle sizes with relatively close protein and fiber contents. These discussed behaviors of powder particles can explain the correlation of protein and fiber enrichment with the average particle size, where protein content increased (Fig. 11a) and fiber content decreased (Fig. 11b) with the rising particle size value.

The SEM images of four fractions in Fig. 12 demonstrated that NCP-T and NCP-B (Fig. 12 a and b) had more spherical-shaped particles accounted for protein bodies than the PCP and CB (Fig. 12 c and d). In addition, several finely milled cell-wall particles comprised the PCP and CB fractions, along with large cotyledon cells with embedded protein bodies.

4. Conclusions

During the tribo-electrostatic separation approach, like the starch-rich legumes, soybean-enriched protein particles were collected from the negatively charged plate (NCP), while the dietary fiber-enriched particles were mainly attracted to the positively charged plate (PCP). The effect of plate voltages (±1, ±3.5, and ±6.5 kV) and air flow rates (7 and 15 LPM) on the fractionation of soybean meal flour was studied during tribo-electrostatic separations. The turbulent flow rate (i.e., 15 LPM) at any tested plate voltage did not result in protein and fiber enrichment in the NCP and PCP fractions. Laminar airflow rate (i.e., 7 LPM) at all tested plate voltages effectively enriched the NCP fractions with protein while only enriching the PCP fractions with fiber at higher plate voltages of ±3.5 and ± 6.5 kV. Increasing plate voltage under both laminar and turbulent conditions enhanced the protein separation efficiency in the NCP fractions with minimal effect on their protein enrichment level. The fiber content and its separation efficiency to PCP fractions improved by increasing the plate voltages under laminar flow but declined under turbulent conditions. Consequently, laminar airflow rate (7 LPM) and high plate voltage (±6.5 kV) were found as those operating conditions that resulted in modest protein and fiber enrichments in the NCP and PCP fractions. At these conditions (7 LPM and ±6.5 kV), the original soybean meal flour with a protein content of 55.3% and fiber content of 15.4% was improved to 58.4% and 19.6%, respectively. Furthermore, 44.4% of the total protein and 16.8% of the total fiber in the original flour were, respectively, recovered in the NCP and PCP fractions after single-stage separation. Higher protein and fiber enrichment levels and their separation efficiencies could be potentially approached through relatively coarse milling of the soybean meal to reduce the cohesive forces between protein and fiber particles during tribo-charging and electrostatic separation. This will provide starting milled flour with a higher D_{V50} than 17.6 μm obtained in this study, which might improve enrichment and separation efficiency. Additionally, the statistical optimization of the tribo-electrostatic separation technique that considers the milling types and intensity along with gas flow rate and plate voltage will help find the optimal enrichment and separation efficiency.

Author statement

Botagoz Kuspangaliyeva: Writing – original draft, Visualization, **Dinara Konakbayeva:** Investigation, Formal analysis, **Solmaz Tabtabaei (Corresponding Author):** Conceptualization, Methodology, Formal analysis, Supervision, Writing- Reviewing and Editing,

Declaration of competing interest

The authors declare that they have no known competing financial interests or personal relationships that could have appeared to influence the work reported in this paper.

Data availability

Data will be made available on request.

Acknowledgments

This project was funded in part through NSF, Grant No. HBCU-UP RIA-1900894 as well as the Provost Office and College of Engineering and Architecture (CEA) at Howard University (Washington, DC).

References

AACC, 2012. Method 08-01.01. In: AACC Approved Methods of Analysis. Cereals & Grains Association, St Paul, MN, USA.

AOAC, 2016. Official Method 922.06. Fat in flour. Acid hydrolysis method. In: Official Methods of Analysis of AOAC International. AOAC International, Gaithersburg, MD, USA.

Basset, C., Kedidi, S., Barakat, A., 2016. Chemical- and solvent-free mechanophysical fractionation of biomass induced by tribo-electrostatic charging: separation of proteins and lignin. ACS Sustain. Chem. Eng. 4, 4166–4173. https://doi.org/10.1021/acssuschemeng.6b00667.

Cangialosi, F., Notarnicola, M., Liberti, L., Stencel, J.M., 2008. The effects of particle concentration and charge exchange on fly ash beneficiation with pneumatic triboelectrostatic separation. Separ. Purif. Technol. 62, 240–248. https://doi.org/10.1016/j.seppur.2008.01.031.

Jafari, M., Rajabzadeh, A.R., Tabtabaei, S., Marsolais, F., Legge, R.L., 2016. Physicochemical characterization of a navy bean (Phaseolus vulgaris) protein fraction produced using a solvent-free method. Food Chem. 208, 35–41. https://doi.org/10.1016/j.foodchem.2016.03.102.

Konakbayeva, D., Kuspangaliyeva, B., Rajabzadeh, A.R., Tabtabaei, S., 2022. Separation behavior of sieved endosperm-enriched oat fractions via tribo-electrostatic approach. Innovat. Food Sci. Emerg. Technol. 80, 103098 https://doi.org/10.1016/j.ifset.2022.103098.

Konakbayeva, D., Tabtabaei, S., 2021. Assessing the chargeability and separability of oat groat particles through sieving combined with triboelectrification-based approach. Separ. Purif. Technol. 278, 119486 https://doi.org/10.1016/j.seppur.2021.119486.

Lee, S.C., Prosky, L., Vries, J.W. De, 1992. Determination of total, soluble, and insoluble dietary fiber in foods—enzymatic-gravimetric method, MES-TRIS buffer: collaborative study. J. AOAC Int. 75, 395–416. https://doi.org/10.1093/jaoac/75.3.395.

Mayr, M.B., Barringer, S.A., 2006. Corona compared with triboelectric charging for electronic powder coating. J. Food Sci. 71 https://doi.org/10.1111/j.1750-3841.2006.00024.x.

Medic, J., Atkinson, C., Hurburgh, C.R., 2014. Current knowledge in soybean composition. JAOCS, J. Am. Oil Chem. Soc. 91, 363–384. https://doi.org/10.1007/s11746-013-2407-9.

Mudgil, D., Barak, S., 2013. Composition, properties and health benefits of indigestible carbohydrate polymers as dietary fiber: a review. Int. J. Biol. Macromol. 61, 1–6. https://doi.org/10.1016/j.ijbiomac.2013.06.044.

Schutyser, M.A.I., van der Goot, A.J., 2011. The potential of dry fractionation processes for sustainable plant protein production. Trends Food Sci. Technol. 22, 154–164. https://doi.org/10.1016/j.tifs.2010.11.006.

Tabtabaei, S., Ataya Pulido, V.M., Diosady, L.L., 2013. Destabilization of yellow mustard emulsion using organic solvents. J. Am. Oil Chem. Soc. 90, 707–716. https://doi.org/10.1007/s11746-013-2202-7.

Tabtabaei, S., Boocock, D.G.B., Diosady, L.L., 2015. Biodiesel production from mustard emulsion by a combined destabilization/adsorption process. J. Am. Oil Chem. Soc. 92, 1205–1217. https://doi.org/10.1007/s11746-015-2677-5.

Tabtabaei, S., Boocock, D.G.B., Diosady, L.L., 2014. Biodiesel feedstock from emulsions produced by aqueous processing of yellow mustard. J. Am. Oil Chem. Soc. 91, 1269–1282. https://doi.org/10.1007/s11746-014-2448-8.

Tabtabaei, S., Diosady, L.L., 2013. Aqueous and enzymatic extraction processes for the production of food-grade proteins and industrial oil from dehulled yellow mustard flour. Food Res. Int. 52, 547–556. https://doi.org/10.1016/j.foodres.2013.03.005.

Tabtabaei, S., Hijar, B., Chen, B.K., Diosady, L.L., 2017a. Functional properties of protein isolates produced by aqueous extraction of de-hulled yellow mustard. J. Am. Oil Chem. Soc. 94, 149–160. https://doi.org/10.1007/s11746-016-2922-6.

Tabtabaei, S., Jafari, M., Rajabzadeh, A.R., Legge, R.L., 2016a. Solvent-free production of protein-enriched fractions from navy bean flour using a triboelectrification-based approach. J. Food Eng. 174, 21–28. https://doi.org/10.1016/j.jfoodeng.2015.11.010.

Tabtabaei, S., Jafari, M., Rajabzadeh, A.R., Legge, R.L., 2016b. Development and optimization of a triboelectrification bioseparation process for dry fractionation of legume flours. Separ. Purif. Technol. 163, 48–58. https://doi.org/10.1016/j.seppur.2016.02.035.

Tabtabaei, S., Konakbayeva, D., Rajabzadeh, A.R., Legge, R.L., 2019. Functional properties of navy bean (Phaseolus vulgaris) protein concentrates obtained by pneumatic tribo-electrostatic separation. Food Chem. 283, 101–110. https://doi.org/10.1016/j.foodchem.2019.01.031.

Tabtabaei, S., Vitelli, M., Rajabzadeh, A.R., Legge, R.L., 2017b. Analysis of protein enrichment during single- and multi-stage tribo-electrostatic bioseparation processes for dry fractionation of legume flour. Separ. Purif. Technol. 176, 48–58. https://doi.org/10.1016/j.seppur.2016.11.050.

Wang, J., De Wit, M., Boom, R.M., Schutyser, M.A.I., 2015a. Charging and separation behavior of gluten-starch mixtures assessed with a custom-built electrostatic separator. Separ. Purif. Technol. 152, 164–171. https://doi.org/10.1016/j.seppur.2015.08.025.

Wang, J., De Wit, M., Schutyser, M.A.I., Boom, R.M., 2014. Analysis of electrostatic powder charging for fractionation of foods. Innovat. Food Sci. Emerg. Technol. 26, 360–365. https://doi.org/10.1016/j.ifset.2014.06.011.

Wang, J., Smits, E., Boom, R.M., Schutyser, M.A.I., 2015b. Arabinoxylans concentrates from wheat bran by electrostatic separation. J. Food Eng. 155, 29–36. https://doi.org/10.1016/j.jfoodeng.2015.01.008.

Wang, J., Zhao, J., De Wit, M., Boom, R.M., Schutyser, M.A.I., 2016. Lupine protein enrichment by milling and electrostatic separation. Innovat. Food Sci. Emerg. Technol. 33, 596–602. https://doi.org/10.1016/j.ifset.2015.12.020.

Xing, Q., de Wit, M., Kyriakopoulou, K., Boom, R.M., Schutyser, M.A.I., 2018. Protein enrichment of defatted soybean flour by fine milling and electrostatic separation. Innovat. Food Sci. Emerg. Technol. 50, 42–49. https://doi.org/10.1016/j.ifset.2018.08.014.